Nonmajor cubic symmetry axes of easy magnetization in rare-earth–iron Laves compounds

U. Atzmony
Nuclear Research Center–Negev, Post Office Box 9001, Beer-Sheva, Israel

M. P. Dariel*
Materials and Molecular Research Division, Lawrence Berkeley Laboratory, Berkeley, California 94720
(Received 16 October 1975)

Unusual $[uuw]$- and $[uv0]$-type axes of easy magnetization have been observed in some cubic rare-earth–iron Laves compounds. The presence of these directions of spontaneous magnetization can be accounted for, within the phenomenological treatment of the magnetic anisotropy, by including eighth-power direction-cosine terms in the power expansion of the magnetic anisotropy energy. It will also be shown that the single-ion model predicts the existence of these directions. The conditions imposed on the bulk magnetic anisotropy constants are derived. Typical values of these constants in rare-earth–iron Laves phases are calculated using the single-ion model.

I. INTRODUCTION

The direction of the spontaneous magnetization reflects the dependence of the magnetic free energy of the crystallographic directions. According to the phenomenological treatment, the magnetic free energy of a cubic crystal can be expanded into a power series of the direction cosines (α_1, α_2, α_3) of the direction of magnetization $\vec{n}$ with respect to the cubic axes:

$$E(\vec{n},\ T) = K_0 + K_1(\alpha_1^2\,\alpha_2^2 + \alpha_2^2\,\alpha_3^2 + \alpha_3^2\,\alpha_1^2) + K_2(\alpha_1^2\,\alpha_2^2\,\alpha_3^2), \quad (1)$$

with $\alpha_1^2 + \alpha_2^2 + \alpha_3^2 = 1$. The K_i's are the temperature-dependent bulk magnetic anisotropy constants. It is commonly accepted that only terms up to the sixth power of the direction cosines should be retained. It can be easily shown by differentiation with respect to the angles β and γ ($\beta = \cos^{-1}\alpha_1$, $\gamma = \cos^{-1}\alpha_2$) that the only minima for $E(\vec{n}, T)$ occur for α_i's corresponding to the major axes of symmetry of the cubic system, namely, the [001], [011], and [111] directions. Which of these becomes an easy axis of magnetization, depends on the relative values of K_1 and K_2. Accordingly, it is generally believed that the crystal-field approach using the single-ion model would yield the same directions of easy magnetization. The Hamiltonian is therefore usually written and solved only for exchange fields, which are assumed to be parallel to the major axes of cubic symmetry.

In recent years Mössbauer-effect studies have been successfully used in order to determine the magnetic anisotropy properties of cubic Laves binary $R\mathrm{Fe}_2$,[1] and ternary $R_x^{(1)}R_{1-x}^{(2)}\mathrm{Fe}_2$ rare-earth–iron compounds.[2,3] In several instances the easy axes of magnetization of these compounds were found to deviate from major cubic directions of symmetry. Such behavior was observed in two main types of compounds: (i) some binary rare-earth–iron Laves compounds CeFe_2,[4] SmFe_2,[5] and HoFe_2,[6] and (ii) ternary mixed-rare-earth $R_x^{(1)}R_{1-x}^{(2)}\mathrm{Fe}_2$ compounds,[7,8] in the course of spin reorientation, which took place upon change of either the composition or the temperature. In most cases the departure of the axis of magnetization from the major axis of symmetry takes place over a relatively broad temperature interval within which $\vec{n}$ rotates continuously over a wide range of directions. This rotation has also been confirmed by means of neutron-diffraction measurements of an oriented powder sample of $\mathrm{Ho}_{0.4}\mathrm{Tb}_{0.6}\mathrm{Fe}_2$.[7] Initially, the unusual directions of magnetization were believed to be due to distortions of the cubic unit cells.

The purpose of the present communication is to show that such cases can be understood within the framework of cubic symmetry. In Sec. II we will show that the presence of K_3, the eighth-power cosine term in the phenomenological expression, yields minima of $E(\vec{n}, T)$ for directions other than the major cubic axes. The analysis allows one to establish the conditions imposed on the bulk magnetic anistropy constants in order that the axis of easy magnetization should deviate from these major axes of symmetry. In Sec. III we will show that the single-ion model, applied to the rare-earth ions, can lead to directions of easy magnetization other than the major cubic axes of symmetry, for various values of the crystal-field parameters. In Sec. IV we shall obtain the values of the magnetic anisotropy constants K_1, K_2, and K_3 for several $R\mathrm{Fe}_2$ compounds and show that K_3 is often of the same order of magnitude as K_1 and K_2. Section V includes a short discussion of some experimental results.

II. PHENOMENOLOGICAL APPROACH

Since the retention of the sixth-power cosine term yields only $E(\vec{n}, T)$ minima associated with the major axes of symmetry, the expression for $E(\vec{n}, T)$ [Eq. (1)] was expanded to include the eighth-power term:

$$E(\vec{n}, T) = K_0 + K_1(\alpha_1^2\alpha_2^2 + \alpha_2^2\alpha_3^2 + \alpha_3^2\alpha_1^2) + K_2(\alpha_1^2\alpha_2^2\alpha_3^2) + K_3(\alpha_1^4\alpha_2^4 + \alpha_2^4\alpha_3^4 + \alpha_3^4\alpha_1^4). \quad (2)$$

The conditions for an extremum in E are

$$\frac{\partial E}{\partial \beta} = \frac{\partial E}{\partial \gamma} = 0. \quad (3)$$

The extremum is a minimum if, at point (β_i, γ_i) which satisfied conditions (3),

$$\frac{\partial^2 E(\beta_i, \gamma_i)}{\partial \beta^2} > 0 \text{ and } \frac{\partial^2 E(\beta_i \gamma_i)}{\partial \gamma^2} > 0, \quad (4a)$$

and the discriminant is positive definite, i.e.,

$$\frac{\partial^2 E(\beta_i, \gamma_i)}{\partial \beta^2}\frac{\partial^2 E(\beta_i, \gamma_i)}{\partial \gamma^2} - \left(\frac{\partial^2 E(\beta_i, \gamma_i)}{\partial \beta\, \partial \gamma}\right)^2 > 0. \quad (4b)$$

Application of conditions (3) and (4) to the first and second derivatives of (2) gives the restrictions imposed on the K_i's in order to obtain minima for E. The results indicate that such minima can exist for directions of $\vec{n}$ parallel to the major axes of symmetry and also for crystallographic directions of type $[uuw]$ $(\beta = \gamma)$ and of type $[uv0]$. These additional directions exist only for $K_3 > 0$. For the sake of conciseness, it is helpful to express K_1 and K_2 in units of K_3, we therefore define $K_1' = K_1/K_3$ and $K_2' = K_2/K_3$. A straightforward calculation (see Appendix) allows one to determine the conditions imposed on the K_i''s which account for the presence of axes of magnetization other than the major axes of symmetry. These conditions for $[uuw]$-type directions are

$$-2 < K_2' < 2 \text{ and } -\tfrac{1}{24}(K_2' + 2)^2 < K_1' < 0$$

or (5a)

$$2 < K_2' < 4 \text{ and } -\tfrac{1}{24}(K_2' + 2)^2 < K_1' < \tfrac{1}{2}(K_2' - 1).$$

The conditions for a $[uv0]$-type direction are

$$0 > K_1' > -\tfrac{1}{2}$$

and (5b)

$$2 < K_2'.$$

Figure 1 represents, in the K_1', K_2' plane, the regions with the different possible axes of magnetization. Within the approximately triangular region ABC, the axis of magnetization is of type $[uuw]$. Within this region $\theta = \cos^{-1}\alpha_3$, defined as the angle between $\vec{n}$ and the [001] axis (see insert, Fig. 1), has values between 0 and 54.4°. Lines of constant θ have been plotted in the ABC region. The angle θ changes continuously across the AB boundary but shows a discontinuity, when crossing the AC or BC boundaries. The cross-hatched region in the neighborhood of A corresponds to a region of local minima of E for $[uuw]$ types of magnetization. Such directions will therefore not be stable. Region CED is similar to ABC, in that

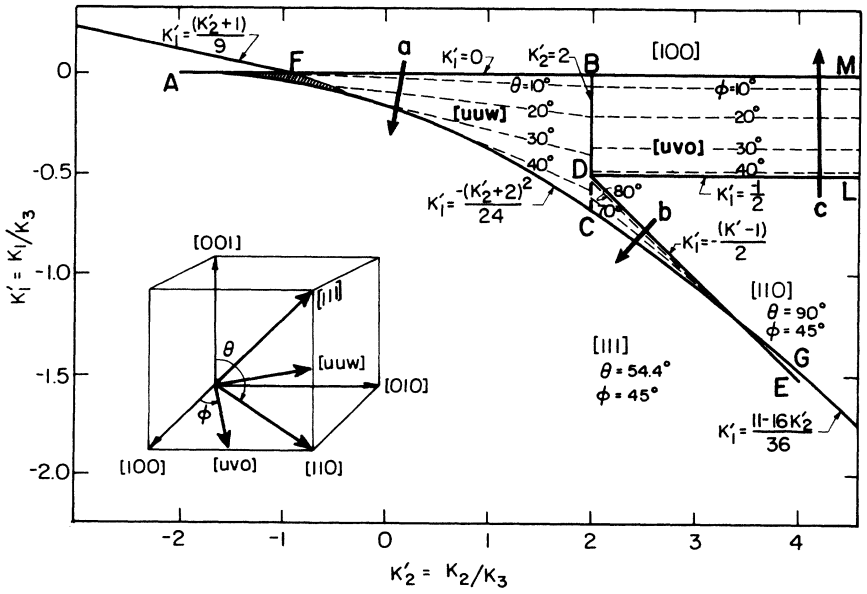

FIG. 1. Boundaries of regions corresponding to different easy axes of magnetization in the $K_1' = K_1/K_3$ and $K_2' = K_2/K_3$ plane. For details see text.

the direction of easy magnetization is of type $[uuw]$, the angle θ within this region varies between 54.4 and 90°. Between points E and G there is again a very narrow band corresponding to nonstable (local minima of E) axes of type $[uuw]$. Region $DBML$ is part of the area in which the direction of magnetization is of type $[uv0]$, i.e., $\theta = 90°$ and $\Phi = \tan^{-1}(v/u)$. Lines of constant Φ have also been plotted in this region, which continues indefinitely towards the right, bounded by the straight lines $K_1' = 0$ and $K_1' = -\frac{1}{2}$.

The variation of the angle θ as function of temperature, deduced from Mössbauer-effect measurements in $CeFe_2$ and $SmFe_2$, is shown in Fig. 2. In $SmFe_2$ the direction of magnetization rotates continuously from the [110] axis at 140 K towards the [111] axis at 240 K. In $CeFe_2$ the axis of magnetization is parallel to the [001] direction up to 150 K; above this temperature it changes to type $[uuw]$ with $\theta \simeq 20°$. Just below the Curie temperature at 230 K, this angle increases to 30°. In $HoFe_2$, $\vec{n}$ is of $[uuw]$ type at $T < 20$ K and parallel to [001] at higher temperatures.[6,8] In some ternary compounds, such as $Ho_{0.5}Er_{0.5}Fe_2$, the behavior is more complex. With increasing temperature the direction of magnetization goes through the sequency $[uuw] \rightarrow [110] \rightarrow [uv0] \rightarrow [100]$.

The phenomenological treatment developed above accounts for all types of behavior. In the case of $CeFe_2$, the values of K_1, K_2, and K_3 vary with increasing temperature in such a way that their projection in the K_1', K_2' plane follows the general trend of the heavy arrow (a) in Fig. 1. For $SmFe_2$ the same projection has the trend of arrow type (b) which crosses region CED going from region [110] towards region [111]. This occurs during the temperature increase from 140 to 240 K. In $Ho_{0.5}Er_{0.5}Fe_2$ the projection follows a direction antiparallel to the arrow of type (b) at low temperatures and thereafter the general direction of the arrow of type (c).

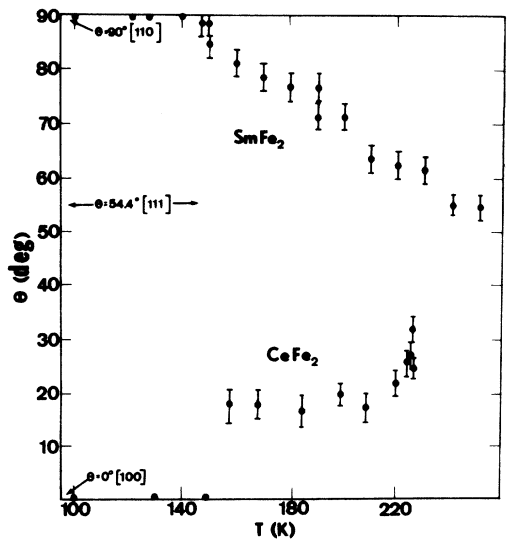

FIG. 2. Temperature dependence of the angle of inclination θ of the direction of easy magnetization with respect to the [001] axis in $CeFe_2$ and $SmFe_2$.

Examination of Fig. 1 also indicates that a spin reorientation involving the [111] direction, namely of type $[111] \rightleftarrows [100]$ or of type $[111] \rightleftarrows [110]$, will not necessarily take place through a transition region, if K_1 and K_2 are sufficiently large, relative to K_3. On the other hand for a $[100] \rightleftarrows [110]$ spin reorientation, there will always be a transition region, with axes of magnetization of type $[uv0]$, even for very small values of the bulk magnetic anisotropy constant K_3.

III. SINGLE-ION APPROACH

The magnetocrystalline anisotropies of rare-earth–containing alloys are attributed mainly to the anisotropy of the interaction between the well-shielded $4f$ electrons of the rare earth with the crystal fields. A detailed discussion of the application of the single-ion-model Hamiltonian to the problem of the anisotropy in rare-earth Laves compounds was given in Ref. 3. The same approach is used here. One finds

$$\mathcal{H}_{\text{anis}} = \sum (\mathcal{H}_{\text{exch}} + \mathcal{H}_{\text{crys}}) = N(\mathcal{H}_{\text{exch}} + \mathcal{H}_{\text{crys}}), \tag{6}$$

with N the number of rare-earth ions per unit volume. The exchange Hamiltonian is

$$\mathcal{H}_{\text{exch}} = 2(g_J - 1)\mu_B H_{\text{exch}} \vec{J} \cdot \vec{n}. \tag{7}$$

In order to take into account a mixing of excited J states into the ground state, V_4 and V_6 were expressed by the Racah operators[9] U_n^m:

$$\mathcal{H}_{\text{crys}} = E_J + V_4 + V_6, \tag{8}$$

where E_J is the energy of the excited state,

$$V_4 = A_4(1 - \sigma_4)\langle r^4 \rangle \left[U_4^0 + (\tfrac{5}{14})^{1/2}(U_4^4 + U_4^{-4})\right], \tag{9a}$$

and

$$V_6 = A_6\langle r^6 \rangle \left[U_6^0 + (\tfrac{7}{2})^{1/2}(U_6^4 + U_6^{-4})\right]. \tag{9b}$$

The values of $\langle r^n \rangle$, the $4f$ radii, and of the shielding factor σ_4 have been calculated by Freeman and Watson.[10,11] A_4 and A_6, the crystal-field parameters, are assumed, as in previous studied,[3] to be independent of the rare-earth ions involved, which are all trivalent. The exchange field H_{exch} was kept constant, $\mu_B H_{\text{exch}} = -150$ K, for all temperatures up to 300 K. Usually $\mathcal{H}_{\text{anis}}$ is calculated and diagonalized for $\vec{n}$ parallel to the three major axes

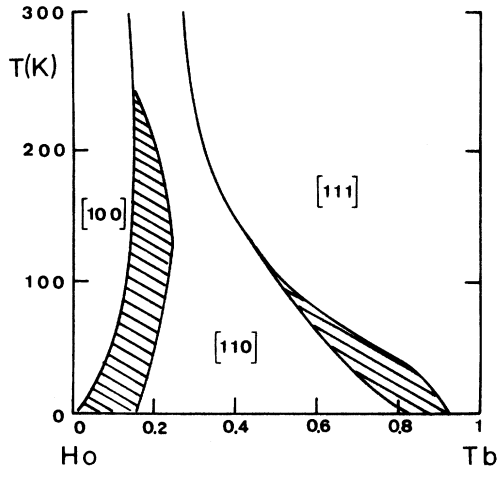

FIG. 3. Spin orientation diagram of the $Tb_x Ho_{1-x} Fe_2$ pseudobinary system. The shaded region corresponds to nonmajor symmetry axes of easy magnetization. The boundaries were calculated using the values $\mu_B H_{exch} = -150$ K, $A_4 = 36$ K/a_0^2, and $A_6/A_4 = -0.038\, a_0^{-2}$.

TABLE I. Direction of $\vec{n}$ for which the magnetic anisotropy Hamiltonian was calculated.

No.	u	v	w
1	0	0	1
2	1	1	10
3	2	2	10
4	3	3	10
5	4	4	10
6	5	5	10
7	6	6	10
8	7	7	10
9	8	8	10
10	9	9	10
11	1	1	1
12	10	10	9
13	10	10	8
14	10	10	7
15	10	10	6
16	10	10	5
17	10	10	4
18	10	10	3
19	10	10	2
20	10	10	1
21	1	1	0
22	10	9	0
23	10	8	0
24	10	7	0
25	10	6	0
26	10	5	0
27	10	4	0
28	10	3	0
29	10	2	0
30	10	1	0

of cubic symmetry. In the present work such calculations are made for thirty different directions of $\vec{n}$, which are confined to the (110) and the (001) planes. These directions, expressed in terms of the indices $[uvw]$, include the major cubic axes of symmetry and are listed in Table I.

The free energy per ion is

$$F_R(\vec{n}_j, T) = -kT \ln Z(\vec{n}_j, T), \tag{10}$$

where $Z(\vec{n}_j, T)$ is the partition function

$$Z(\vec{n}_j, T) = \sum_{i=1}^{m} e^{-E_i/kT}, \tag{11}$$

where the E_i are eigenvalues and m is the number of energy levels,

$$m = 2J + 1. \tag{12}$$

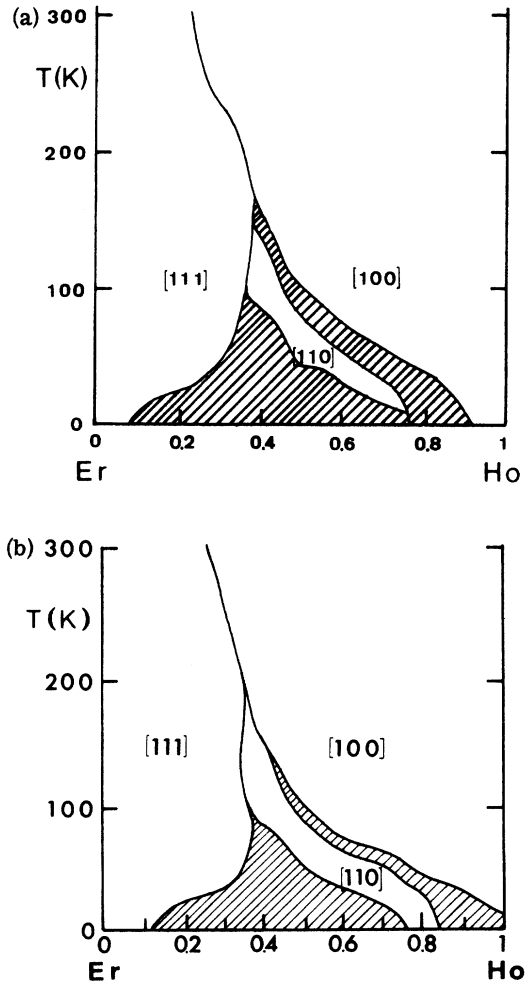

FIG. 4. Spin orientation diagram of the $Ho_x Er_{1-x} Fe_2$ pseudobinary system: (a) parameters as in Fig. 3; (b) $A_6/A_4 = -0.043 a_0^{-2}$; other parameters as in Fig. 3.

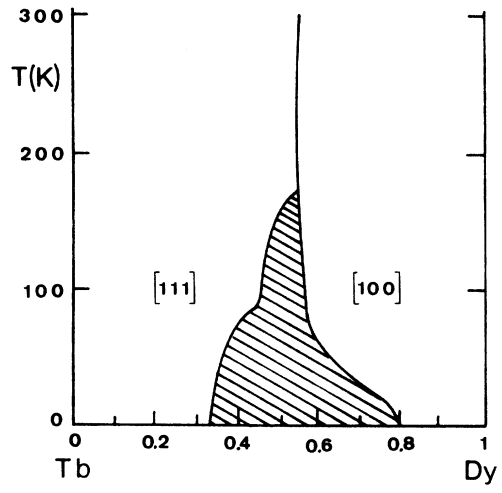

FIG. 5. Spin orientation diagram of the $Dy_x Tb_{1-x} Fe_2$ pseudobinary system. Parameters as in Fig. 3.

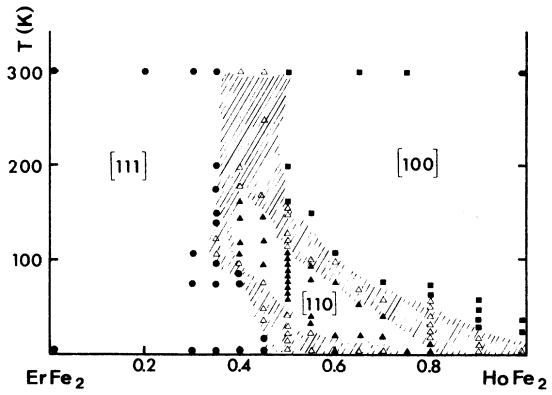

FIG. 7. Experimental spin orientation diagram of the $Ho_x Er_{1-x} Fe_2$ system (Refs. 6 and 8) to be compared to the theoretical diagrams of Fig. 4. Solid circles, triangles, and squares correspond to Mössbauer spectra characteristic of the [111], [011], and [001] easy directions of magnetization, respectively. Open triangles stand for Mössbauer spectra identified as being due to $[uuw]$- or $[uv0]$-type directions of easy magnetization.

For a ternary combination $R_x^1 R_{1-x}^2$ the magnetocrystalline free energy is expressed by

$$F(x, \vec{n}_j, T) = x F_{R^1}(\vec{n}_j, T) + (1-x) F_{R^2}(\vec{n}_j, T). \tag{13}$$

The easy direction of magnetization of a given composition at a given temperature is the direction of $\vec{n}_j$ for which the free energy has its lowest value. This procedure when repeated for various values of x and T is used to construct spin orientation diagrams (SOD). In the present calculations values of $A_4 = 36$ K$/a_0^2$ and $A_6/A_4 = -0.038 a_0^{-2}$ (a_0 is the radius of Bohr) were used. These values were found to yield theoretical SOD's in good agreement with the experimental SOD's.[3] Spin orientation diagrams thus calculated for various $R^{(1)} - R^{(2)}$ combinations with $R^{(1)}$ = Ho, Dy, and $R^{(2)}$ = Tb, Er are shown in Figs. 3–6. These SOD's clearly exhibit the presence of "unusual" directions of easy magnetization (shaded areas in Figs. 3–6), that is, directions not parallel to the major cubic symmetry axes, for all the investigated $R^{(1)} - R^{(2)}$ systems. It should be noted that in the Ho-Tb and Ho-Er systems, regions which correspond to all three major axes of cubic symmetry are obtained. In

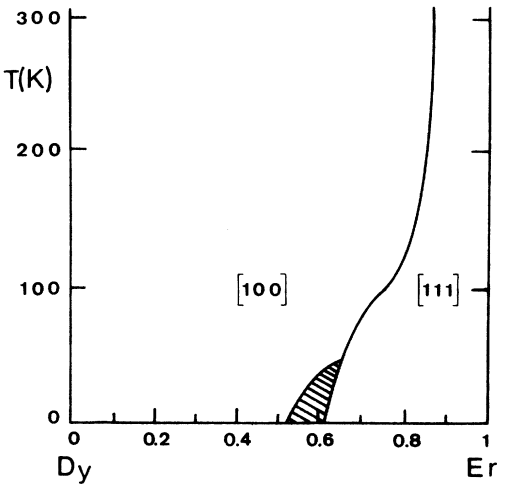

FIG. 6. Spin orientation diagram of the $Er_x Dy_{1-x} Fe_2$ pseudobinary system. Parameters as in Fig. 3.

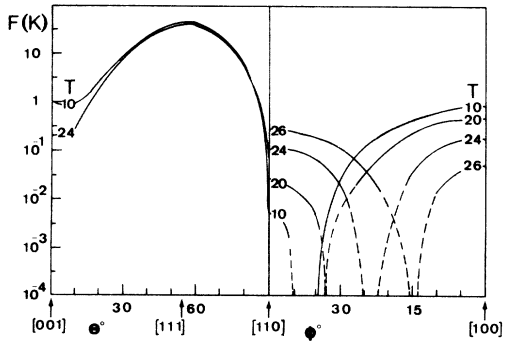

FIG. 8. Magnetic anisotropy free energy F (with respect to its minimal value) of Ho^{+3} in $HoFe_2$ as a function of the direction of magnetization within the $(1\bar{1}0)$ and the (001) plane at several temperatures, $\mu_B H_{exch} = -150$ K, $A_4 = 36$ K$/a_0^2$, and $A_6/A_4 = -0.045 a_0^{-2}$.

the Dy-Tb and Dy-Er systems however, only regions of the [100] and [111] type are present. The experimental SOD of[6] $Ho_xEr_{1-x}Fe_2$ is shown in Fig. 7. For the elemental rare-earths involved, as is seen in Figs. 3–6, $\vec{n}$ is parallel to one single major axis of cubic symmetry. As mentioned above, in $HoFe_2$ the direction of easy magnetization was observed to deviate from the [100] direction below 20 K.[6] This behavior can be accounted for by slightly increasing A_6/A_4 [Fig. 4(b)]. The results obtained for Ho^{3+} (in $HoFe_2$) with $\mu_B H_{\text{exch}} = -150$ K, $A_4 = 36$ K/a_0^2, and $A_6/A_4 = -0.045a_0^{-2}$ are shown in Fig. 8. In this figure, the relative values of the magnetic anisotropy free energy F (with respect to its minimum value) are plotted as a function of the direction of magnetization $\vec{n}$ at various temperatures. In the left-hand part of the figure, $\vec{n}$ is confined to the $(1\bar{1}0)$ plane, in the right-hand part $\vec{n}$ is in the (001) plane. Clearly the minimum of F corresponds to $\vec{n}$ lying in the (001) plane. With increasing temperature $\vec{n}$ rotates towards the [100] direction. The temperature dependence of $\phi = \tan^{-1}(u/v)$ is shown in Fig. 9.

IV. BULK ANISOTROPY CONSTANTS

The bulk magnetic anisotropy constants can be derived from the single-ion magnetic anisotropy free energy $F_R(\vec{n}_j, T)$ using the expression

$$F_R(\vec{n}_j, T) = K_0 + K_1(\alpha_1^2\alpha_2^2 + \alpha_2^2\alpha_3^2 + \alpha_3^2\alpha_1^2) + K_2(\alpha_1^2\alpha_2^2\alpha_3^2) + K_3(\alpha_1^4\alpha_2^4 + \alpha_2^4\alpha_3^4 + \alpha_3^4\alpha_1^4). \quad (14)$$

In order to illustrate the relative importance of the K_3 term, the procedure described as follows was employed. Diagonalization of the Hamiltonian for the different $\vec{n}_j$ $(j = 1, 30)$ directions yielded 30 corresponding independent $F_R(\vec{n}_j, T)$ values at a given temperature. These values were used in order to determine by least-squares fitting of (14), two sets of K_i's, one for $i = 0, 1, 2$ and the second for $i = 0, 1, 2, 3$. The two sets of K_i's can be resubstituted in Eq. (14) to calculate for any $\vec{n}_j$, two corresponding values of the anisotropy energy $E(\vec{n}_j, T)$. These values calculated by truncating the power expansion after three and four terms, respectively, are compared to $F_R(\vec{n}_j, T)$. In all instances the agreement between $E(\vec{n}_j, T)$ and $F_R(\vec{n}_j, T)$ is improved by an order of magnitude when the K_3 term is included in the power-series expansion. As the temperature increases, the relative importance of the K_3 term rapidly decreases. The anisotropy constants $K_i(T)$, $i = 1, 2, 3$ in units of K/ion are plotted as a function of temperature for the trivalent Dy, Ho, Tb, and Er ions in Figs. 10–13. These K_i's were obtained using $\mu_B H_{\text{exch}} = 150$ K, $A_4 = 36$ K/a_0^2, and $A_6/A_4 = -0.038a_0^{-2}$. For Ho^{3+} the K_i's for $A_6/A_4 = -0.045a_0^{-2}$ are also plotted, but only K_1 is affected by the change of A_6/A_4. Several points of interest should be noted. (i) K_3 is found to be positive for all investigated R^{3+} ions. (ii) K_3 is of the same order of magnitude as K_1 and K_2 at low temperatures, but decreases faster with increasing temperatures. (iii) K_1 in Ho^{3+} and K_2 in Dy^{3+} change signs as the temperature is increased.

In order to obtain $[uuw]$- or $[uv0]$-type easy axes of magnetization the calculated K_i's $(i = 1, 2, 3)$ have to satisfy conditions (5a) and (5b) of Sec. II.

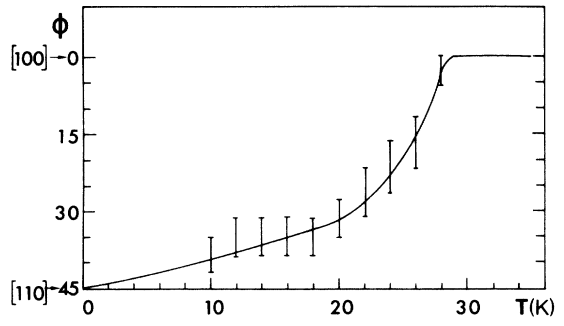

FIG. 9. Temperature dependence of ϕ (the angle between $\vec{n}$ and the [100] axis) for $HoFe_2$. Values of parameters the same as those of Fig. 8.

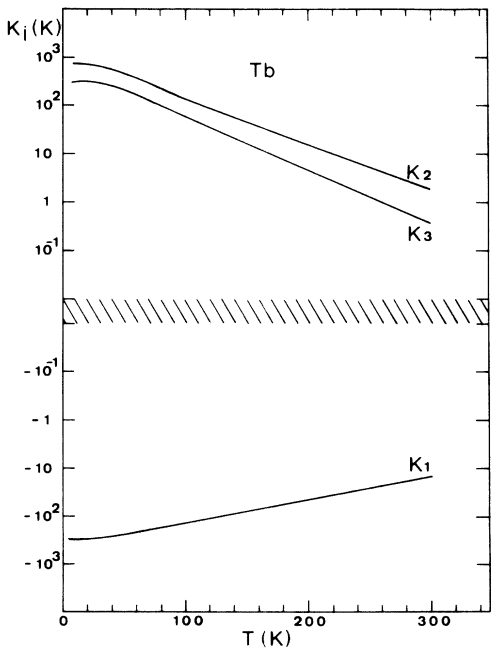

FIG. 10. Bulk magnetic anisotropy constants of Tb^{+3} in $TbFe_2$, parameters as in Fig. 3. The K_i's are plotted on a logarithmic scale in units of K/ion. The shaded region corresponds to values $-10^{-2} \leq K_i \leq 10^{-2}$.

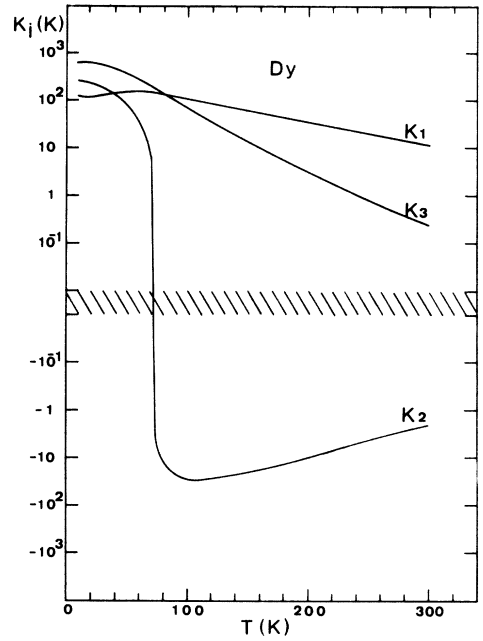

FIG. 11. Bulk magnetic anisotropy constants of Dy^{+3} in $DyFe_2$, parameters as in Fig. 3. Remark as referred to in Fig. 10.

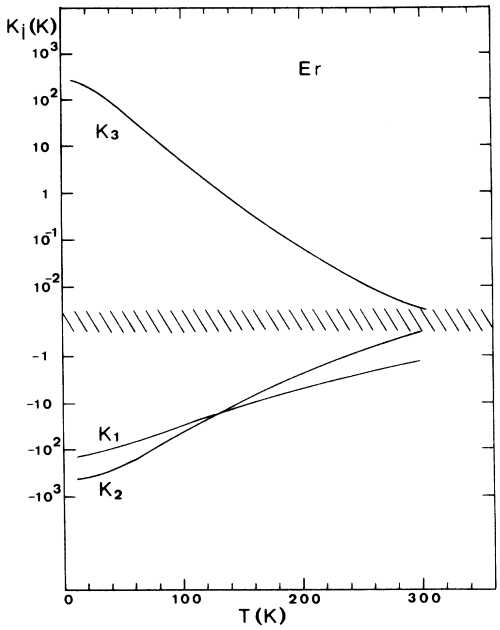

FIG. 13. Bulk magnetic anisotropy constants of Er_2^{+3} in $ErFe_2$, parameters as in Fig. 3. Remark as referred to in Fig. 10.

For a ternary Laves compound, $R_x^{(1)}R_{1-x}^{(2)}Fe_2$, we assume $K_i = xK_{i,R^{(1)}} + (1-x)K_{i,R^{(2)}}$. It is found that the calculated K_i's do satisfy conditions (5a) and (5b) at elevated T. At low T slight deviations from these conditions are observed. It should be noted that both conditions (5a) and (5b) and the calculated K_i's have been derived for a free energy which is expanded up to the eighth order of the cosine terms. Considering also that the relative importance of the K_3 term increases by a few orders of magnitude as T decreases to 4.2 K, it is not implausible that higher cosine terms in the expansion of $E(\vec{n}, T)$ may become significant at low temperatures.

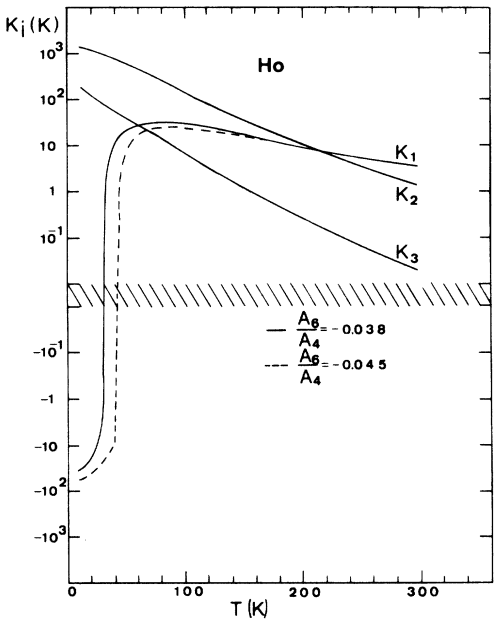

FIG. 12. Bulk magnetic anisotropy constants of Ho^{+3} in $HoFe_2$, parameters as in Fig. 3. Remark as referred to in Fig. 10.

V. DISCUSSION

In the previous sections we have shown that the existence of nonmajor symmetry axes of easy magnetization in cubic crystals is not in contradiction with the cubic symmetry and that actually such axes can be predicted by the crystal-field single-ion model. It should be emphasized at this point that the single-ion Hamiltonian of the rare-earth elements is not the only source of the experimentally observed magnetic anisotropy. This is quite clear in $CeFe_2$, $LuFe_2$,[4] and YFe_2,[1] which exhibit magnetic anisotropy, but where it is obviously not due to the single-ion rare earth, but probably to the iron sublattice. A further complication is the minute rhombohedral distortion reported in $TbFe_2$,[12] which is due to the extremely strong magnetoelastic interactions. No similar distortions have, however, been observed in other RFe_2 compounds.

In the phenomenological treatment of the magnetic anisotropy, the presence of nonmajor symmetry axes of spontaneous magnetization can be accounted for by including higher-order direction-cosine terms. A non-negligible K_3 term has been observed in the course of careful torque measurements in Ni metal.[13] It is not implausible that for certain values of K_i's ($i = 0, 1, 2, 3, 4$) axes of spontaneous magnetization parallel to general $[uvw]$ directions might be observed. This will give rise to four inequivalent iron sites in RFe_2 compounds. The Mössbauer spectra in such cases[3,4,6] would be a superposition of four six-line patterns. This however, will be hardly detectable from the experimental data, even though mathematically the quality of the theoretical fits will improve as the number of superimposed spectra increases from three to four.

Recently Williams and Koon[14] reported the results of bulk magnetic anisotropy constants measurements on a single crystal of $Tb_{0.15}Ho_{0.85}Fe_2$ using torque magnetometry techniques. In general their findings are in satisfactory agreement with the SOD of the (Ho-Tb)Fe_2 system as determined on the basis of Mössbauer spectroscopy and calculated using the single-ion model. Williams and Koon were unable to observe a triple point which indeed does not appear in the corrected SOD of Fig. 3. Following the usual procedure, Williams and Koon neglected higher than sixth-power cosine terms in the analysis of their experimental results. Neglecting eighth-power terms is justified at $T > 150$ K, it is not however, according to our results, at lower temperatures. The discrepancy at higher temperatures between their measured K_i's and those calculated in the present work is not too surprising. Torque measurements yield values of the over-all bulk anisotropy constants irrespective of their microscopic origin, while our calculations determined only the contribution of the single rare-earth–ion anisotropy to those constants.

VI. CONCLUSIONS

Inclusion of the eighth-power cosine terms in the phenomenological expansion of the magnetic anisotropy free energy accounts for the presence of $[uuv]$- and $[uv0]$-type spontaneous axes of magnetization. The presence of such axes has been observed in several binary and ternary rare-earth–iron cubic compounds.

The single-ion model predicts the existence of such nonmajor cubic symmetry axes of easy magnetization.

The value of the bulk magnetic anisotropy constant K_3 is of the same order as those of K_1 and K_2 at low temperature, but decreases faster with increasing temperature.

ACKNOWLEDGMENTS

Fruitful discussions with Professor M. Weger are gratefully acknowledged. One of us (M.P.D.) acknowledges the support of the U. S. Energy Research and Development Administration.

APPENDIX

Starting with Eq. (2), substituting $\alpha_3^2 = 1 - \alpha_1^2 - \alpha_2^2$, changing the notation to $\alpha_1 = \cos\beta$ and $\alpha_2 = \cos\gamma$ and applying conditions (3) for the extremum, we obtain

$$\frac{\partial E}{\partial \beta} = 2\sin\beta\cos\beta\,(2\cos^2\beta - 1 + \cos^2\gamma) \times [K_1 + K_2\cos^2\gamma - 2K_3\,(\cos^4\beta - \cos^2\beta + \cos^2\beta\cos^2\gamma + \cos^4\gamma)] = 0\,,$$

$$\frac{\partial E}{\partial \gamma} = 2\sin\gamma\cos\gamma\,(2\cos^2\gamma - 1 + \cos^2\beta) \times [K_1 + K_2\cos^2\beta - 2K_3\,(\cos^4\gamma - \cos^2\gamma + \cos^2\gamma\cos^2\beta + \cos^4\beta)] = 0\,.$$

Each derivative is a product of four factors. These derivatives will simultaneously satisfy conditions (3) whenever one of the four factors (not necessarily the same in the two expressions) will vanish. We distinguish several cases.

Case 1. $\cos\beta = \cos\gamma = 0$, $\cos\beta = \sin\gamma = 0$, or $\sin\beta = \cos\gamma = 0$. This case corresponds to the $\langle 100\rangle$ axes of magnetization.

Case 2.

$$\cos\beta = 0 \text{ and } 2\cos^2\gamma - 1 + \cos^2\beta = 0$$

or

$$\cos\gamma = 0 \text{ and } 2\cos^2\beta - 1 + \cos^2\gamma = 0\,.$$

This corresponds to the $\langle 110\rangle$ axes of magnetization.

Case 3.

$$2\cos^2\gamma - 1 + \cos^2\beta = 0$$

and

$$2\cos^2\beta - 1 + \cos^2\gamma = 0\,.$$

This corresponds to the $\langle 111\rangle$ axes of magnetization.

Substituting the values of $\cos\beta$ and $\cos\gamma$ in each case into the quadratic form, Eq. (4b), yields the limiting values of K_1' and K_2' (assuming $K_3 > 0$) for which the above-mentioned major axes of sym-

metry become easy axes of magnetization.

Case 4. The nonmajor axes of easy magnetization are obtained by the vanishing of the second and fourth factors, respectively, in the two derivatives; i.e.

$$\cos\beta = 0$$

and

$$K_1 + K_2\cos^2\beta - 2K_3\,(\cos^4\gamma - \cos^2\gamma + \cos^2\beta\cos^2\gamma + \cos^4\beta) = 0\,.$$

This yields the $\langle uv0\rangle$ directions, the angle ϕ between the direction of magnetization and the [100] axis being in this case $\sin^2 2\phi = \sin^2 2\beta = -2K_1/K_3$ (again $K_3 > 0$). The magnetic anisotropy free energy E_{uv0} is equal to $-\frac{3}{4}K_1^2/K_3$.

Case 5. Finally the vanishing of the third factor in one derivative and the fourth in the second or the vanishing of both fourth factors, i.e.,

$$2\cos^2\beta - 1 + \cos^2\gamma = 0$$

and

$$K_1 + K_2\cos^2\beta - 2K_3\,(\cos^4\gamma - \cos^2\gamma + \cos^2\gamma\cos^2\beta + \cos^4\beta) = 0\,,$$

or

$$K_1 + K_2\cos^2\gamma - 2K_3\,(\cos^4\beta - \cos^2\beta + \cos^2\beta\cos^2\gamma + \cos^4\gamma) = 0$$

and

$$K_1 + K_1\cos^2\beta - 2K_3\,(\cos^4\gamma - \cos^2\gamma + \cos^2\beta\cos^2\gamma + \cos^4\beta) = 0$$

yields the minima for the $\langle uuw\rangle$ directions. The angle θ (see Fig. 1) in this case is $\theta = \cos^{-1}(1 - 2\cos^2\beta)$ and

$$\cos\beta = \{(K_2 + 2K_3) + [(K_2 + 2K_3)^2 + 24\,K_1K_3]^{1/2}\}/12K_3\,.$$

Substituting in (3) and taking into account that $1 \geq \cos^2\beta \geq 0$ we obtain the boundaries of region *ABDGECA* in Fig. 1. The expression for the energy in this case is complicated. Numerical computations show that in the shaded area near *A* and in the narrow strip between *G* and *E*, the minima for a $[uuw]$ direction are local minima only or, in other words, in these regions the magnetic anisotropy free energy has lower values for the magnetization lying along a major symmetry axis.

---

*Visiting scientist on leave from the Nuclear Research Center–Negev, and the Department of Materials Engineering, Ben-Gurion University of the Negev, Beer-Sheva, Israel.

[1]G. T. Bowden, D. St. P. Bunbury, A. P. Guimaraes, and R. E. Snyder, J. Phys. C 1, 1376 (1968).

[2]U. Atzmony, M. P. Dariel, E. R. Bauminger, D. Lebenbaum, I. Nowik, and S. Ofer, Phys. Rev. Lett. 28, 244 (1972).

[3]U. Atzmony, M. P. Dariel, E. R. Bauminger, D. Lebenbaum, I. Nowik, and S. Ofer, Phys. Rev. B 7, 4220 (1973).

[4]U. Atzmony and M. P. Dariel, Phys. Rev. B 10, 2060 (1974).

[5]U. Atzmony, M. P. Dariel, E. R. Bauminger, D. Lebenbaum, I. Nowik, and S. Ofer, Proceedings of the Tenth Rare-Earth Conference, Carefree, Arizona, 1973 (unpublished), p. 605.

[6]M. Rosen, H. Klimker, U. Atzmony, and M. P. Dariel, J. Phys. Chem. Solids (to be published).

[7]G. Dublon, U. Atzmony, M. P. Dariel, and H. Shaked, Phys. Rev. B 12, 4628 (1975).

[8]U. Atzmony and M. P. Dariel, AIP Conf. Proc. 24, 662 (1974).

[9]M. J. Weber and R. W. Bierig, Phys. Rev. 134, A1492 (1964).

[10]A. J. Freeman and R. E. Watson, Phys. Rev. 127, 2058 (1962).

[11]A. J. Freeman and R. E. Watson, Phys. Rev. 139, A1606 (1965).

[12]A. E. Dwight and C. W. Kimball, Acta Crystallogr. B30, 2791 (1972).

[13]G. Aubert, J. Appl. Phys. 39, 504 (1968).

[14]C. W. Williams and N. C. Koon, Phys. Rev. B 11, 4360 (1975).